


 Cite this: *RSC Adv.*, 2020, 10, 17836

# Microwave roasting of blast furnace slag for carbon dioxide mineralization and energy analysis†

 Zike Han,<sup>a</sup> Jianqiu Gao,<sup>a</sup> Xizhi Yuan,<sup>a</sup> Yanjun Zhong,<sup>a</sup> Xiaodong Ma,<sup>b</sup> Zhiyuan Chen,<sup>c</sup> Dongmei Luo<sup>a</sup> and Ye Wang<sup>id</sup>\*<sup>a</sup>

For both the waste treatment of large quantities of blast furnace (BF) slag and carbon dioxide (CO<sub>2</sub>) that are discharged in ironworks, mineral carbonation by BF slag was proposed in this decade. However, it has not been widely used due to its high energy consumption and low production efficiency. In this study, a microwave roasting method was employed to mineralize CO<sub>2</sub> with BF slag, and the process parameters for the sulfation and energy consumption were investigated. A mixture of BF slag and recyclable ammonium sulfate [(NH<sub>4</sub>)<sub>2</sub>SO<sub>4</sub>] (mass ratio, 1 : 2) was roasted in a microwave tube furnace, and then leached with distilled water at a solid : liquid ratio of 1 : 3 (g mL<sup>-1</sup>). Under the optimized experiment conditions (*T* = 340 °C, holding time = 2 min), the best sulfation ratios of calcium (Ca), magnesium (Mg), aluminum (Al), and titanium (Ti) were 93.3%, 98.3%, 97.5%, and 80.4%, respectively. Compared with traditional roasting, the production efficiency of this process was more than 10 times higher, and the energy consumption for mineralizing 1 kg of CO<sub>2</sub> could be reduced by 40.2% after simulation with Aspen Plus v8.8. Moreover, 236.1 kg of CO<sub>2</sub> could be mineralized by one ton of BF slag, and a series of by-products with economic value could also be obtained. The proposed process offers an energy-efficient method with high productivity and good economy for industrial waste treatment and CO<sub>2</sub> storage.

Received 28th March 2020

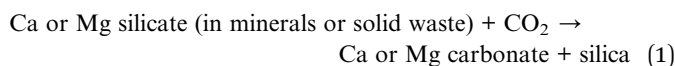
Accepted 20th April 2020

DOI: 10.1039/d0ra02846k

[rsc.li/rsc-advances](http://rsc.li/rsc-advances)

## 1. Introduction

The reduction of carbon dioxide (CO<sub>2</sub>) emissions is a global problem related to the sustainable development of human society. The storage technology of CO<sub>2</sub> can be divided into geologic storage, ocean storage, and mineralization.<sup>1</sup> The mineralization technology has the advantages of a mild, safe reaction and stable products for the spontaneous reaction. For most minerals and some solid wastes (steel slag, coal slag, *etc.*), it can be given in a simplified form as:



In 2018, global crude steel production was 1.808 billion tons, and 723 million tons of blast furnace (BF) slag were produced accordingly. Based on the mathematical model proposed by Ba-Shammakh,<sup>2</sup> 2.1 tons of CO<sub>2</sub> per ton of crude steel will be produced; that is, 5.25 tons of CO<sub>2</sub> will be generated for each ton

of BF slag production. As the CO<sub>2</sub> capture potential of BF slag can be 413 ± 13 kg CO<sub>2</sub> per ton,<sup>3</sup> mineral carbonation by BF slag was proposed to treat large quantities of steel industry waste: BF slag and CO<sub>2</sub>.<sup>4</sup> Ca and Mg in BF slag were used to mineralize CO<sub>2</sub> and a series of by-products with economic value can be obtained.<sup>5</sup> The primary limiting factor of the mineralization process is the low productivity and economic efficiency.<sup>6</sup>

The extraction of Ca and Mg from BF slag is the key technology in the mineralization process. Both hydrometallurgical and pyrometallurgical methods have been reported with some extractants, such as acetic acid,<sup>7</sup> ammonium acetate,<sup>8</sup> hydrochloric acid,<sup>9</sup> sulfuric acid,<sup>10,11</sup> ammonium bisulfate,<sup>12-14</sup> ammonium sulphate,<sup>15,16</sup> and mono-ethanolamine.<sup>17</sup> In the hydrometallurgical method, Eloneva *et al.*<sup>7</sup> used acetic acid to leach Ca and Mg from BF slag. To mineralize 1 kg of CO<sub>2</sub>, 4.4 kg of BF slag, 3.6 L of acetic acid, and 3.5 kg of sodium hydroxide (NaOH) were consumed. However, the high power consumption for the regeneration of NaOH made the process unsuitable for CO<sub>2</sub> storage. Chu *et al.*<sup>18</sup> proposed a completely wet process, whereby sulfuric acid (H<sub>2</sub>SO<sub>4</sub>) and (NH<sub>4</sub>)<sub>2</sub>SO<sub>4</sub> were mixed to generate ammonium bisulfate (NH<sub>4</sub>HSO<sub>4</sub>), and then BF slag was leached in NH<sub>4</sub>HSO<sub>4</sub> solution at 80 °C in 20 min. The mass ratio of BF slag to NH<sub>4</sub>HSO<sub>4</sub> was 1 : 3.25, and the leaching ratios of Ca, Mg, and Al reached 97.3%, 98.8%, and 96.4%, respectively. However, the corrosion of equipment and its unsuitability for Ti-bearing BF slag restrict the improvement of this

<sup>a</sup>School of Chemical Engineering, Sichuan University, No. 24 South Section 1, Yihuan Road, Chengdu 610065, P. R. China. E-mail: wangye@scu.edu.cn

<sup>b</sup>School of Chemical Engineering, University of Queensland, Brisbane, Australia

<sup>c</sup>Department of Materials Science and Engineering, Delft University of Technology, The Netherlands

† Electronic supplementary information (ESI) available. See DOI: 10.1039/d0ra02846k



method. In pyrometallurgical roasting, Hu *et al.*<sup>19</sup> used  $(\text{NH}_4)_2\text{SO}_4$  to replace the high-cost  $\text{NH}_4\text{HSO}_4$  as a recycling extractant, and the sulfation ratios of Ca, Mg, and Al were close to 100%. Compared with ordinary BF slag, the components of Ti-bearing BF slag are more difficult to be sulfated. Wang *et al.*<sup>20</sup> roasted  $(\text{NH}_4)_2\text{SO}_4$  and Ti-bearing BF slag at 350 °C for 2 h and leached with dilute sulfuric acid. The sulfation ratios of Ca, Mg, Al, and Ti were 85%, 92.6%, 84.4%, and 87%, respectively. Whereas, the traditional roasting method needs to be heated for more than 2 h, which means a low production efficiency and high energy consumption.

To improve the production efficiency and reduce the energy consumption, microwave roasting technology was employed to mineralize  $\text{CO}_2$  with BF slag for two reasons: one, the Ti-bearing BF slag has a good microwave absorption performance in this process, and two, a larger microwave reactor has been developed that is more feasible for realizing industrialization. Moreover, with the existence of calcium titanate ( $\text{CaTiO}_3$ ), Ti-bearing BF slag is more difficult to sulfate than ordinary BF slag. In this study, microwave technology was used to extract valuable elements, such as Ca, Mg, Al, Fe, and Ti, from Ti-bearing BF slag with high efficiency. Ca and Mg can be used to mineralize  $\text{CO}_2$ . Meanwhile, a series of by-products with economic value can also be obtained, such as titanium dioxide ( $\text{TiO}_2$ ) and ammonium alum ( $\text{NH}_4\text{-Al}(\text{SO}_4)_2 \cdot 12\text{H}_2\text{O}$ ). The findings will be useful in reducing the energy consumption of  $\text{CO}_2$  mineralization and for enhancing the production efficiency of solid waste treatment, whereby the  $\text{CO}_2$  emission from steel and iron industry can be reduced. Moreover, this method is also expected to be applied to the  $\text{CO}_2$  mineral carbonation of other wastes.

## 2. Materials and methods

### 2.1 Materials

In this study, the BF slag was supplied by Panzhihua Iron and Steel Group Co., Ltd., including ordinary BF slag and water-quenched Ti-bearing BF slag. Moreover, the following chemicals were used in the experiment: analytically pure  $(\text{NH}_4)_2\text{SO}_4$  and  $\text{H}_2\text{SO}_4$  (Chengdu Kelong Reagent Co., Ltd.) and nitrogen ( $\text{N}_2$ , Chengdu Xuyuan Chemical Engineering Co., Ltd.) with a purity of >99.99%.

In order to identify the phase analysis, X-ray diffraction (DX-1000, Dandong Oriental Circle Instrument Co., Ltd., China) was used, with a copper target ( $\lambda = 0.154056$  nm) used as the target, test range of  $2\theta = 10\text{--}80^\circ$ , tube voltage of 40 kV, and tube current of 40 mA. The elemental composition of BF slag was investigated by X-ray fluorescence spectrometry (XRF-1800, Shimadzu, Japan), with a Rh target used as the target.

In addition, the microstructure of the BF slag and leaching residue were observed by scanning electron microscopy (SEM, JSM-7500F, Japan Electronics Corporation, Japan) at an accelerating voltage of 10 kV. The relative elemental content of leaching residue was analyzed with combined energy-dispersive X-ray spectrometry (EDS, IS250, Oxford Instrument Company, UK). To measure the Ca, Mg, Al, and Ti concentrations in the leaching solution, inductively coupled plasma optical emission spectroscopy (ICP-OES, Spectro ARCOS ICP, Germany) was used.

To perform the energy analysis, Aspen Plus software v8.8 was applied to simulate the whole process. However, since the Aspen database lacks some thermodynamic data for some species, the missing thermodynamic data were retrieved from the HSC Chemistry 6.0 database. It is worthy to mention that the simulations of the  $\text{CO}_2$  capture and the mineralization process were based on our previous research.<sup>8,21–23</sup>

### 2.2 Experimental apparatus

Microwave roasting technology was employed in mineralizing  $\text{CO}_2$  with BF slag. The energy loss of the microwave in unit volume of material<sup>22</sup> is:

$$P = 2\pi f \epsilon' \epsilon'' E^2 \quad (2)$$

where  $P$  ( $\text{W m}^{-3}$ ) is the power density of microwave absorbed by the materials;  $f$  (Hz) is the microwave frequency;  $\epsilon'$  is the dielectric constant;  $\epsilon''$  is the dielectric loss factor; and  $E$  ( $\text{V m}^{-1}$ ) is the electric field strength. The ability for absorbing microwaves increased with the  $P$ -value, which reflects the selectivity of the microwave heating.<sup>23–25</sup> The dielectric constant and dielectric loss of the main materials were measured by a network analyzer and probe method (5071C, Shide Technologies Co., Ltd., China), over the testing frequency range from 1 to 18 GHz.

A microwave tube furnace (Fig. 1, HY-ZG, Hunan Huaie Microwave Technology Co., Ltd.) was applied to proceed with the experimental procedure. A cylinder of pressurized  $\text{N}_2$  was attached to the quartz tube, and the injection rate of the inlet gas was measured by a rotameter ( $\text{LZB-3}$ , 60–600  $\text{mL min}^{-1}$ ). The infrared thermometer, which was located on the top of the tube furnace, was used to measure the temperature, and the temperature interval set in this study was between 25–50 °C for reducing the error.<sup>26</sup> In order to determine the range of temperature, the temperature dependence of the Gibbs free energy of the main reactions ( $\text{R}_1\text{--R}_5$  from Table 1) during microwave roasting are shown in Fig. 2, with these thermodynamic data retrieved from the HSC Chemistry 6.0 database. The standard Gibbs free energy change of  $\text{R}_1$ ,  $\text{R}_2$ ,  $\text{R}_3$ ,  $\text{R}_4$ , and  $\text{R}_5$  become negative from 200 °C, 100 °C, 200 °C, 200 °C, and 300 °C, respectively. Therefore, the experimental temperature range was set from 210 °C to 400 °C.

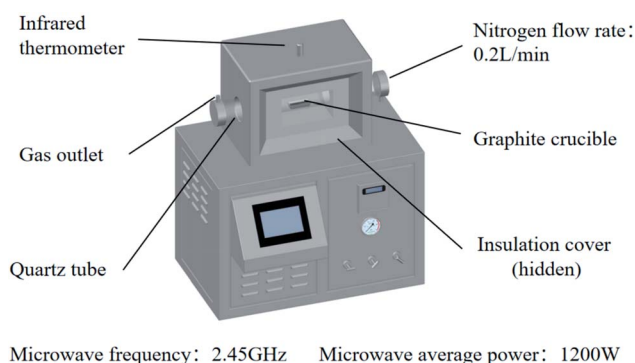


Fig. 1 Schematic of the microwave tube furnace.



Table 1 The reactions in the microwave roasting of Ti-bearing BF slag

No.	Reactions
R <sub>1</sub>	$\text{CaMgSi}_2\text{O}_6(\text{s}) + 2(\text{NH}_4)_2\text{SO}_4(\text{l}) \rightarrow \text{CaSO}_4(\text{s}) + \text{MgSO}_4(\text{s}) + 2\text{SiO}_2(\text{s}) + 4\text{NH}_3(\text{g}) + 2\text{H}_2\text{O}(\text{g})$
R <sub>2</sub>	$\text{CaAl}_2\text{SiO}_6(\text{s}) + 4(\text{NH}_4)_2\text{SO}_4(\text{l}) \rightarrow \text{CaSO}_4(\text{s}) + \text{Al}_2(\text{SO}_4)_3(\text{s}) + \text{SiO}_2(\text{s}) + 8\text{NH}_3(\text{g}) + 4\text{H}_2\text{O}(\text{g})$
R <sub>3</sub>	$\text{Ca}_3\text{Al}_2\text{O}_6 + 6(\text{NH}_4)_2\text{SO}_4(\text{l}) \rightarrow 3\text{CaSO}_4(\text{s}) + \text{Al}_2(\text{SO}_4)_3(\text{s}) + 6\text{H}_2\text{O}(\text{g}) + 12\text{NH}_3(\text{g})$
R <sub>4</sub>	$\text{CaTiO}_3(\text{s}) + 2(\text{NH}_4)_2\text{SO}_4(\text{l}) \rightarrow \text{CaSO}_4(\text{s}) + \text{TiOSO}_4(\text{s}) + 4\text{NH}_3(\text{g}) + 2\text{H}_2\text{O}(\text{g})$
R <sub>5</sub>	$(\text{NH}_4)_2\text{SO}_4(\text{l}) \rightarrow \text{NH}_4\text{HSO}_4(\text{l}) + \text{NH}_3(\text{g})$
R <sub>6</sub>	$\text{MO}(\text{s}) + (\text{NH}_4)_2\text{SO}_4(\text{l}) \rightarrow \text{MSO}_4(\text{s}) + \text{H}_2\text{O}(\text{g}) + 2\text{NH}_3(\text{g})$ (M = Mg or Ca)
R <sub>7</sub>	$2\text{TiOSO}_4(\text{s}) \rightarrow 2\text{TiO}_2(\text{s}) + 2\text{SO}_2(\text{g}) + \text{O}_2(\text{g})$

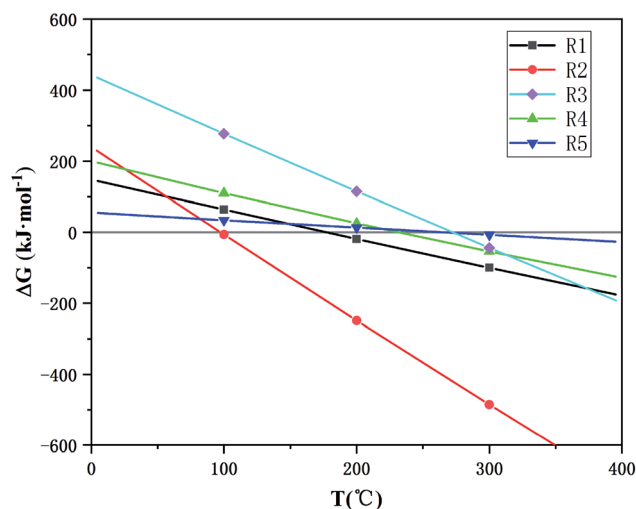


Fig. 2 The temperature dependence of Gibbs free energy of the main reaction during microwave roasting.

### 2.3 Experimental procedure

The experimental procedure in this study included two parts: microwave roasting and leaching. First, BF slag (100 mesh), ground by an agate mortar, was mixed uniformly with  $(\text{NH}_4)_2\text{SO}_4$  at a mass ratio of 1 : 2, and then placed in a graphite crucible. The crucible was placed in a microwave tube furnace with a microwave frequency of 2.45 GHz, and average microwave power of 1200 W (at 340 °C). After several minutes of heating and a few minutes of heat preservation, the power supply was turned off and  $\text{N}_2$  was fed until the sample was cooled below 30 °C and then removed. The ammonia ( $\text{NH}_3$ ) generated during the reaction was absorbed by distilled water. The roasted product was leached with distilled water at a solid : liquid ratio of 1 : 3 ( $\text{g mL}^{-1}$ ) for 1 h at 55 °C. The leached slurry was filtered and separated to obtain a leaching residue rich in calcium sulfate ( $\text{CaSO}_4$ ) and silica ( $\text{SiO}_2$ ) and a leaching solution rich in magnesium, aluminum, and titanium sulfates.

Table 2 Chemical composition of the BF slag

Composition	O	Ca	Ti	Si	Al	Mg	Fe	Others
Ti-bearing BF slag	42.81%	18.24%	<b>11.88%</b>	11.3%	5.63%	4.07%	2.08%	3.99%
BF slag	40.75%	27.33%	<b>0.47%</b>	16.39%	6.98%	6.09%	1.03%	0.96%

A direct leaching experiment was conducted to confirm the enhancement effect of the microwave roasting method. A mixture of BF slag and  $(\text{NH}_4)_2\text{SO}_4$  (mass ratio, 1 : 2) was leached directly with 10%  $\text{H}_2\text{SO}_4$  at a solid : liquid ratio of 1 : 3 ( $\text{g mL}^{-1}$ ) without microwave roasting, where the sulfation ratios of Mg, Al, and Ti were 49.6%, 25.2%, and 10.1%, respectively.

According to R<sub>1</sub>–R<sub>4</sub> in Table 1 and the compositions in Table 2, BF slag and  $(\text{NH}_4)_2\text{SO}_4$  have a theoretical mass ratio of 1 : 1.624. However, the actual mass ratio of BF slag to  $(\text{NH}_4)_2\text{SO}_4$  was 1 : 2, because an excess  $(\text{NH}_4)_2\text{SO}_4$  can not only promote the sulfation of BF slag, but also decompose into  $\text{NH}_4\text{HSO}_4$  during microwave roasting process. With the help of  $\text{NH}_4\text{HSO}_4$ , the acidity of the solution can be increased, the consumption of sulfuric acid can be reduced, and the hydrolysis of  $\text{Ti}^{4+}$  can be inhibited during leaching. After microwave roasting and leaching, most of the Ca is transferred into the leaching residue in the form of  $\text{CaSO}_4$ . Based on the composition of raw materials, the sulfation ratio of Ca is positively correlated with that of Mg, Al, and Ti. Therefore, only the sulfation ratios of Mg, Al, and Ti under different conditions were analyzed to determine the optimized microwave roasting conditions.

### 2.4 Calculation of the sulfation ratios

Since  $\text{CaSO}_4$  is slightly soluble in water,  $\text{CaSO}_4$  was also present in the leaching solution. The concentrations of  $\text{Ca}^{2+}$ ,  $\text{Mg}^{2+}$ ,  $\text{Al}^{3+}$ , and  $\text{Ti}^{4+}$  in the leaching solution obtained under different roasting conditions were determined by ICP-OES. For determining the content of  $\text{CaSO}_4$  in the leaching residue, 0.500 g of leaching residue was dissolved in 250 mL distilled water at room temperature, and then the content of Ca in the solution was determined by ICP-OES.

The sulfation ratios of Mg, Al, Ti ( $S_{\text{Mg}}$ ,  $S_{\text{Al}}$ ,  $S_{\text{Ti}}$ ) were calculated using eqn (3):

$$S_i = (c_i \times V) / (m_1 \times w_i) \times 100\% \quad (3)$$

where  $c_i$  ( $\text{g L}^{-1}$ ) is the concentration of  $\text{Mg}^{2+}$ ,  $\text{Al}^{3+}$ ,  $\text{Ti}^{4+}$  in the leaching solution;  $V$  (L) is the volume of the leaching solution;



$m_1$  (g) is the quality of BF slag obtained in each experiment; and  $w_1$  (wt%) is the mass fraction of Mg, Al, Ti in the BF slag.

The sulfation ratio of Ca ( $S_{Ca}$ ) was calculated using eqn (4):

$$S_2 = (c_2 \times V + m_2 \times w_2) / (m_1 \times w_3) \times 100\% \quad (4)$$

where  $c_2$  ( $\text{g L}^{-1}$ ) is the concentrations of  $\text{Ca}^{2+}$  in the leaching solution;  $m_2$  (g) is the quality of the leaching residue;  $w_2$  (wt%) is the mass fraction of Ca in the form of  $\text{CaSO}_4$  in the leaching residue; and  $w_3$  (wt%) is the mass fraction of Ca in the BF slag.

## 3. Results and discussion

### 3.1 Physicochemical characterization of the BF slag

The chemical composition of the slag was analyzed by XRF, and the results are shown in Table 2. The results show that the content of Ti in the Ti-bearing BF slag was 11.88%, which has a high recycling value. A higher content of Ca and Mg is beneficial to the mineralization of  $\text{CO}_2$ , whereby according to the content of Ca and Mg, it can be calculated that the  $\text{CO}_2$  capture potential of the Ti-bearing BF slag was 274.0 kg  $\text{CO}_2$  per ton (see ESI†). Furthermore, Al and Fe in the slag can be recovered in the subsequent process.

The microstructure of BF slag observed by SEM is shown in Fig. 3. There is little difference in appearance between Ti-bearing BF slag and ordinary BF slag, which are irregular granular, where the particle size of treated Ti-bearing BF slag is less than 0.15 mm. According to the different cooling systems, BF slag can be divided into water-quenched slag and slow-cooling slag. Compared with slow-cooling slag, the particle size of water-quenched slag is much smaller and it is easy to crush. However, BF slag is quenched into a glassy, amorphous form. After nucleation at  $780^\circ\text{C}$  for 1.5 h and crystallization at  $850^\circ\text{C}$  for 2 h, XRD was performed and the analysis results are shown in Fig. 4, with the main constituents in the BF slag being perovskite ( $\text{CaTiO}_3$ ), calcium aluminate ( $\text{Ca}_3\text{Al}_2\text{O}_6$ ), diopside ( $\text{Ca}(\text{Mg},\text{Al})(\text{Si},\text{Al})_2\text{O}_6$ ),  $\text{Ca}(\text{Mg},\text{Fe},\text{Al})(\text{Si},\text{Al})_2\text{O}_6$ ,  $\text{Ca}(\text{Ti},\text{Mg},\text{Al})(\text{Si},\text{Al})_2\text{O}_6$ , and calcium silicate ( $\text{CaSiO}_3$ ).

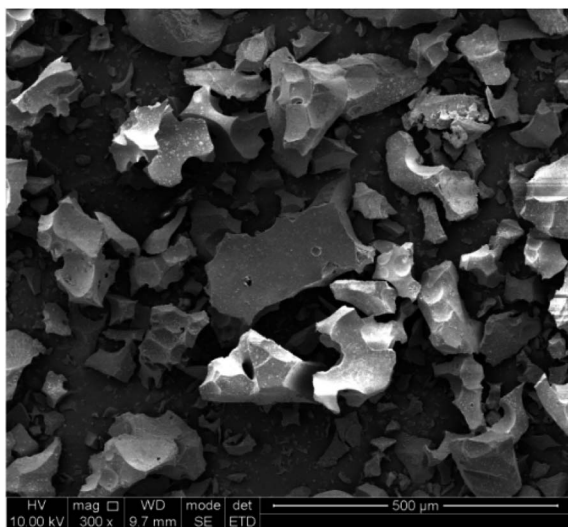


Fig. 3 SEM image of the Ti-bearing BF slag.

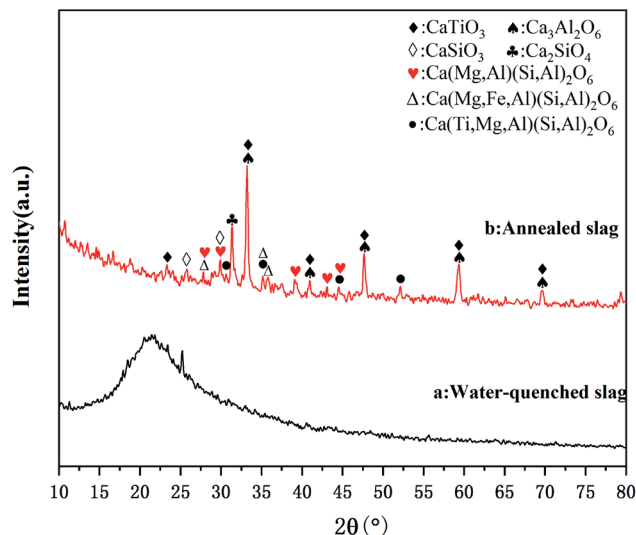


Fig. 4 XRD patterns of the Ti-bearing BF slag before (a) and after (b) annealing at  $850^\circ\text{C}$ .

### 3.2 Characterization of the leaching residue

To understand the composition of the leaching residue and the reason for the low  $S_{\text{Ti}}$ , the leaching residue was characterized by SEM. The morphology of the leaching residue is shown in Fig. 5(a). Dendritic and massive crystals and amorphous powders could be seen in the slag. Fig. 5(b) is a partial enlargement of Fig. 5(a). Combined with the EDS analysis results and XRD pattern in Fig. 6, it can be seen that the dendritic crystal in Fig. 5(b) is  $\text{CaSO}_4$ , the bulk crystal is  $\text{SiO}_2$ , a small amount of powder is  $\text{CaTiO}_3$ . There was also a large number of amorphous powders, the main component of which is  $\text{CaSO}_4$ , whereby most of the Ca in Ti-bearing BF slag is transferred into the leaching residue. A small amount of  $\text{CaTiO}_3$  also appeared in the leaching residue, which is one of the reasons for the low  $S_{\text{Ti}}$  in this process. However, as the leaching residue may contain a small amount of amorphous titanium dioxide (produced by the decomposition of  $\text{CaTiO}_3$ ), the specific content of  $\text{CaTiO}_3$  was not obtained.

### 3.3 Effect of the roasting temperature

In the study of the effect of the roasting temperature on the sulfation of the elements in BF slag, BF slag and  $(\text{NH}_4)_2\text{SO}_4$  were mixed uniformly at a mass ratio of 1 : 2. The mixture was heated to the corresponding temperature in a microwave tube furnace, and kept there for 2 min (optimized holding time obtained in Section 3.4); then cooled to room temperature and leached with distilled water at a solid : liquid ratio of 1 : 3 ( $\text{g mL}^{-1}$ ) for 1 h at  $55^\circ\text{C}$ . The sulfation ratios of Mg, Al, and Ti at different roasting temperatures are shown in Fig. 7. After microwave roasting,  $S_{\text{Mg}}$  was close to 100% at  $210^\circ\text{C}$ , while Mg existed in the form of  $\text{CaMgSi}_2\text{O}_6$  in the BF slag (as shown in Fig. 4), and the  $\Delta G$  of  $R_1$  at  $210^\circ\text{C}$  from Fig. 2 was consistent with the experimental results. In this process,  $S_{\text{Ti}}$  was still 10.2% before  $300^\circ\text{C}$ , which indicated that  $\text{CaTiO}_3$  did not react with  $(\text{NH}_4)_2\text{SO}_4$  under this condition. The XRD pattern of the roasted products at different



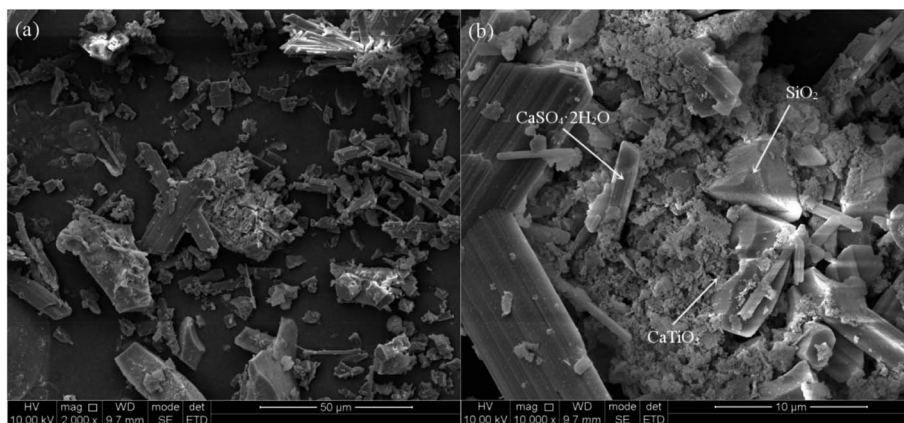


Fig. 5 SEM image of the leaching residue (a) and its magnified view (b).

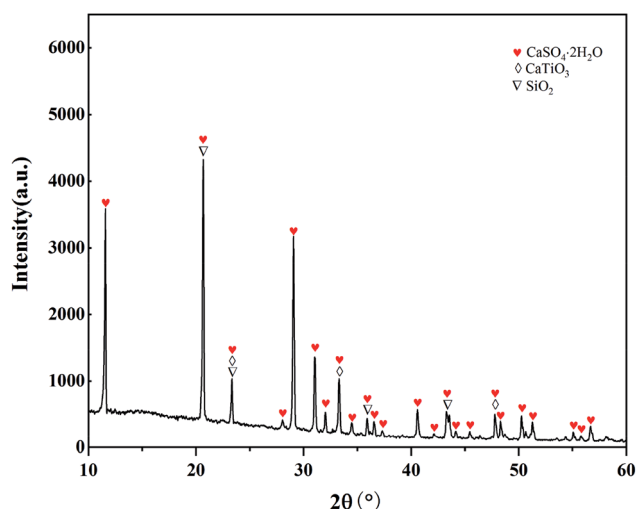


Fig. 6 XRD pattern of the leaching residue.

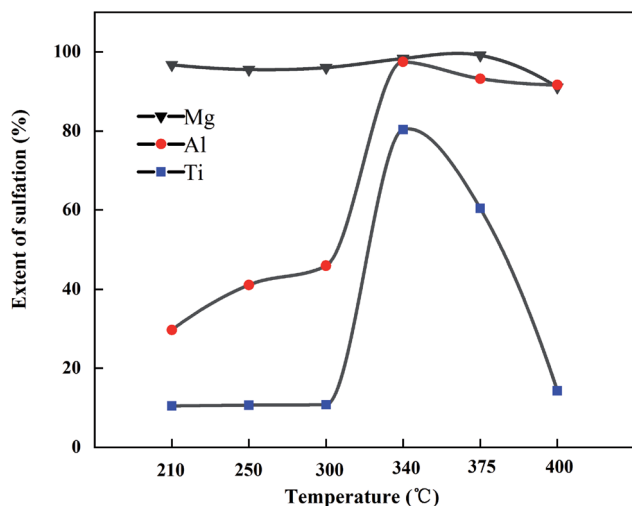


Fig. 7 The effect of roasting temperature on the sulfation of Mg, Al, and Ti (roasting: holding time 2 min, AS: slag mass ratio of 2 : 1; leaching: distilled water, solid : liquid ratio of 1 : 3 (g mL<sup>-1</sup>), 55 °C, 1 h).

temperatures is shown in Fig. 8 (there was no CO<sub>2</sub> in the microwave process, so the carbonation reaction will be carried out in the mineralization process). From Fig. 8, when the temperature rose to 300 °C, the intermediate (NH<sub>4</sub>)<sub>3</sub>H(SO<sub>4</sub>)<sub>2</sub> was formed, meanwhile, *S*<sub>Al</sub> and *S*<sub>Ti</sub> rose sharply under this condition. The sulfation ratio reached the maximum at 340 °C; at this point, the crystalline compositions of the product were NH<sub>4</sub>-Fe(SO<sub>4</sub>)<sub>2</sub>, CaSO<sub>4</sub>, and (NH<sub>4</sub>)<sub>3</sub>H(SO<sub>4</sub>)<sub>2</sub>. Beyond 340 °C, *S*<sub>Ti</sub> decreased with the increase in temperature. When the temperature rose to 400 °C, *S*<sub>Ti</sub> was 14.3%, which was close to the *S*<sub>Ti</sub> before microwave roasting – this was attributed to thermal runaway.<sup>27</sup>

In this study, the dielectric constant and loss of main materials were measured by a network analyzer and probe method, as shown in Table 3, where it can also be seen that the dielectric constant and loss of roasted raw materials were similar to that of (NH<sub>4</sub>)<sub>2</sub>SO<sub>4</sub>, and the dielectric constant of Ti-bearing BF slag was about twice that of (NH<sub>4</sub>)<sub>2</sub>SO<sub>4</sub>. The dielectric constant and loss of CaTiO<sub>3</sub> were much larger than that of other substances in the experiment. The *P*-value of CaTiO<sub>3</sub> was

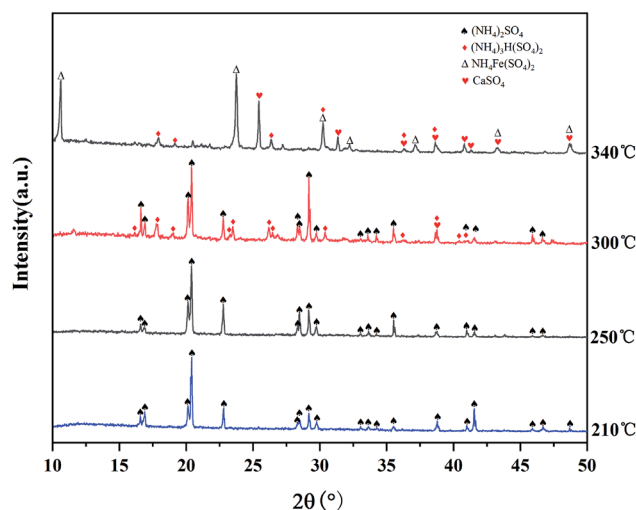


Fig. 8 XRD patterns of the roasting products obtained at different roasting temperatures (holding time: 2 min).



Table 3 Permittivity and dielectric loss of the main materials

Material	$\epsilon'$ (permittivity)	$\epsilon''$ (dielectric loss)
Ti-bearing BF slag	8.40	0.123
$(\text{NH}_4)_2\text{SO}_4$	3.38	0.132
$\text{CaTiO}_3$ (ref. 27)	130	1.364
Roasted materials <sup>a</sup>	3.98	0.142

<sup>a</sup>  $(\text{NH}_4)_2\text{SO}_4$  was mixed with Ti-bearing BF slag at a mass ratio of 2 : 1.

much larger than other substances in the experiment so that it was easier to be heated. The electric and thermal fields produced by the microwave in the Ti-bearing BF slag were not uniform, because the Ti element in the Ti-bearing BF slag existed in the form of  $\text{CaTiO}_3$ , whereby the different absorbing ability led to the nonuniform temperature distribution. The dielectric loss of  $\text{CaTiO}_3$  increased with the roasting temperature, resulting in a thermal runaway around  $\text{CaTiO}_3$ , whereby  $\text{TiOSO}_4$  was decomposed into  $\text{TiO}_2$  ( $R_7$  in Table 1), which was difficult to react with dilute sulfuric acid, thus leading to the decrease in  $S_{\text{Ti}}$ . The two Ti-related reactions in this process are shown in Table 1 as  $R_4$  and  $R_6$ .

In the resistance furnace, the first step of  $(\text{NH}_4)_2\text{SO}_4$  decomposition to produce  $\text{NH}_4\text{HSO}_4$  mainly occurs at  $>250^\circ\text{C}$ .<sup>28</sup> In this work, the XRD peak of  $(\text{NH}_4)_3\text{H}(\text{SO}_4)_2$  appeared at  $300^\circ\text{C}$ , indicating that the  $(\text{NH}_4)_2\text{SO}_4$  began to decompose. The peak of  $(\text{NH}_4)_2\text{SO}_4$  disappeared and  $\text{NH}_4\text{Fe}(\text{SO}_4)_2$  began to appear when the temperature rose to  $340^\circ\text{C}$ . Moreover,  $(\text{NH}_4)_2\text{SO}_4$  can react fully with minerals at this temperature, as seen from Fig. 7.

It should be noted that the sulfation ratio reached about 95% after 7 min of heating and 2 min of holding time using microwave roasting; whereas under the traditional roasting conditions, the sulfation ratio of ordinary BF slag in the first 10 min was lower,<sup>29</sup>  $S_{\text{Mg}}$  and  $S_{\text{Al}}$  were about 50% and about 5%, respectively. The conversion of Ti-bearing BF slag in the first 10 min was much lower.<sup>30</sup> It was obvious that the reaction rate of microwave roasting was much faster than that of traditional roasting.

### 3.4 Effect of the holding time

In the study of the effect of different holding times on the sulfation of the elements in BF slag, BF slag and  $(\text{NH}_4)_2\text{SO}_4$  were mixed uniformly at a mass ratio of 1 : 2. The sulfation ratios of Mg, Al, and Ti at different holding times are shown in Fig. 9. Under this condition,  $S_{\text{Mg}}$  was close to 100%, and  $S_{\text{Ti}}$  was about 10%. When the holding time was 1 min,  $S_{\text{Al}}$  was over 80%, and  $S_{\text{Ca}}$  began to increase. When the holding time was 2 min,  $S_{\text{Mg}}$ ,  $S_{\text{Al}}$ , and  $S_{\text{Ti}}$  all reached the maximum.  $S_{\text{Ca}}$  in the leaching residue was determined under this condition, and the sulfation ratios of Ca, Mg, Al, and Ti were 93.3%, 98.3%, 97.5%, and 80.4%, respectively.

After 2 min of heat preservation,  $S_{\text{Mg}}$  and  $S_{\text{Al}}$  tended to be stable with the increase in time, with figures close to 100%. Affected by the phenomenon of "thermal runaway",  $S_{\text{Ti}}$  decreased sharply with the increase in holding time, and the

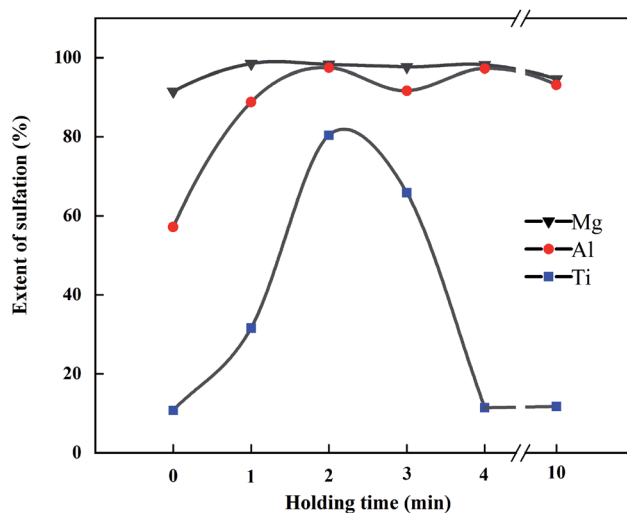


Fig. 9 The effect of different holding times on the sulfation of Mg, Al, and Ti (roasting: temperature  $340^\circ\text{C}$ , AS : slag mass ratio of 2 : 1; leaching: distilled water, solid : liquid ratio of 1 : 3 ( $\text{g mL}^{-1}$ ),  $55^\circ\text{C}$ , 1 h).

color of the product transitioned from black to white; whereby when the holding time exceeded 4 min, the color of the product completely turned white. The decomposition product  $\text{TiO}_2$  does not react with dilute sulfuric acid, thus resulting in a decrease in  $S_{\text{Ti}}$ .

As can be seen from Fig. 10, the only crystalline substance in the raw material was  $(\text{NH}_4)_2\text{SO}_4$ . There were no new diffraction peaks during heating from room temperature to  $340^\circ\text{C}$ . The diffraction peaks of  $(\text{NH}_4)_2\text{SO}_4$  disappeared after 2 min of heat preservation at  $340^\circ\text{C}$ , and the main crystalline components of the product were  $(\text{NH}_4)_3\text{H}(\text{SO}_4)_2$  and  $(\text{NH}_4)_3\text{Fe}(\text{SO}_4)_3$ . After 2 min of heat preservation, the diffraction peaks of  $(\text{NH}_4)_3\text{Fe}(\text{SO}_4)_3$  disappeared and the peaks of  $\text{NH}_4\text{Fe}(\text{SO}_4)_2$  and  $\text{CaSO}_4$  appeared. It could be inferred that the following reactions took place:

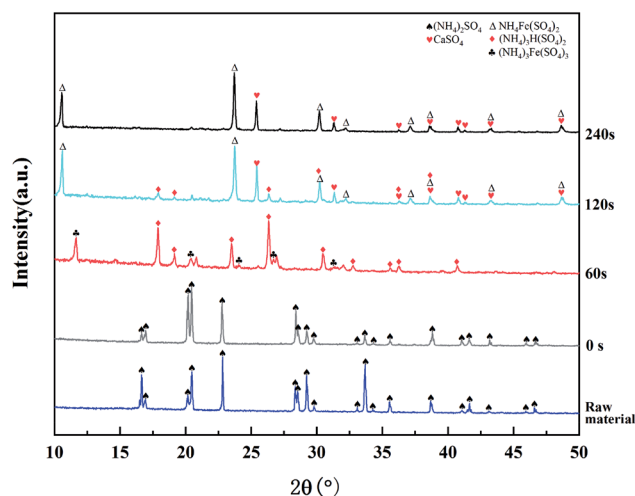
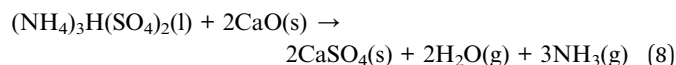
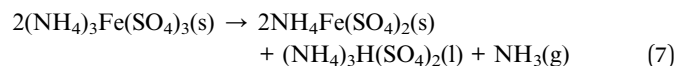
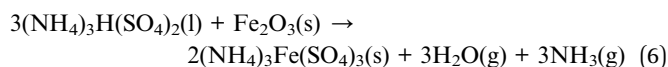
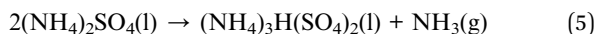


Fig. 10 XRD patterns of the roasting products obtained at different holding times (roasting temperature:  $340^\circ\text{C}$ ).





When the holding time was extended to 4 min, the peak of  $(\text{NH}_4)_3\text{H}(\text{SO}_4)_2$  disappeared, indicating that it had been completely decomposed, and the  $S_{\text{Ti}}$  clearly decreased. The decomposition reaction of  $\text{TiOSO}_4$  and  $(\text{NH}_4)_3\text{H}(\text{SO}_4)_2$  was unfavorable for the process, because it not only reduced the yield of Ti, but also increased the consumption of acid in the leaching process. Therefore, the optimized holding time was 2 min.

## 4. Energy analysis

Based on the above analysis, it can be concluded that the microwave roasting process has a shorter roasting time and higher sulfation ratio than the traditional roasting process. Therefore, the treatment efficiency of BF slag can be

significantly improved. In order to further illustrate the advantages of the process in terms of the energy consumption, based on the experimental results and previous experimental data, the processes of microwave roasting and traditional roasting were simulated by Aspen Plus v8.8 software, respectively, and the energy consumption of the microwave roasting process was analyzed. The whole process could be divided into six steps as shown in Fig. 11. The main chemical reaction equations involved in the process are shown in Table 1. The specific process material relations are listed in Fig. 12.

Combined with Fig. 11 and 12, the whole process is as follows:

Step 1: A mixture of BF slag and  $(\text{NH}_4)_2\text{SO}_4$  was roasted in the microwave tube furnace at 340 °C for 2 min.

Step 2: The roasted material was leached at a solid : liquid ratio of 1 : 3 ( $\text{g ml}^{-1}$ ), and the leaching process was carried out in a water bath at 55 °C and the leaching time was 1 h. The leaching solution was acidic due to the  $\text{NH}_4\text{HSO}_4$  decomposed by excessive  $(\text{NH}_4)_2\text{SO}_4$ , so  $\text{Ti}^{4+}$  did not hydrolyze. It is worth mentioning that the roasting products in this process were leached with water instead of dilute sulfuric acid, compared with previous studies,<sup>20</sup> so about 57 kg sulfuric acid per ton of BF slag could be saved.

Step 3: The leaching solution was hydrolyzed at 102 °C for 4 h, and  $\text{Ti}^{4+}$  was precipitated in the form of  $\text{TiO}_2 \cdot \text{H}_2\text{O}$ . 186.3 kg of  $\text{TiO}_2 \cdot \text{H}_2\text{O}$  could be obtained with 1 ton of BF slag, and after

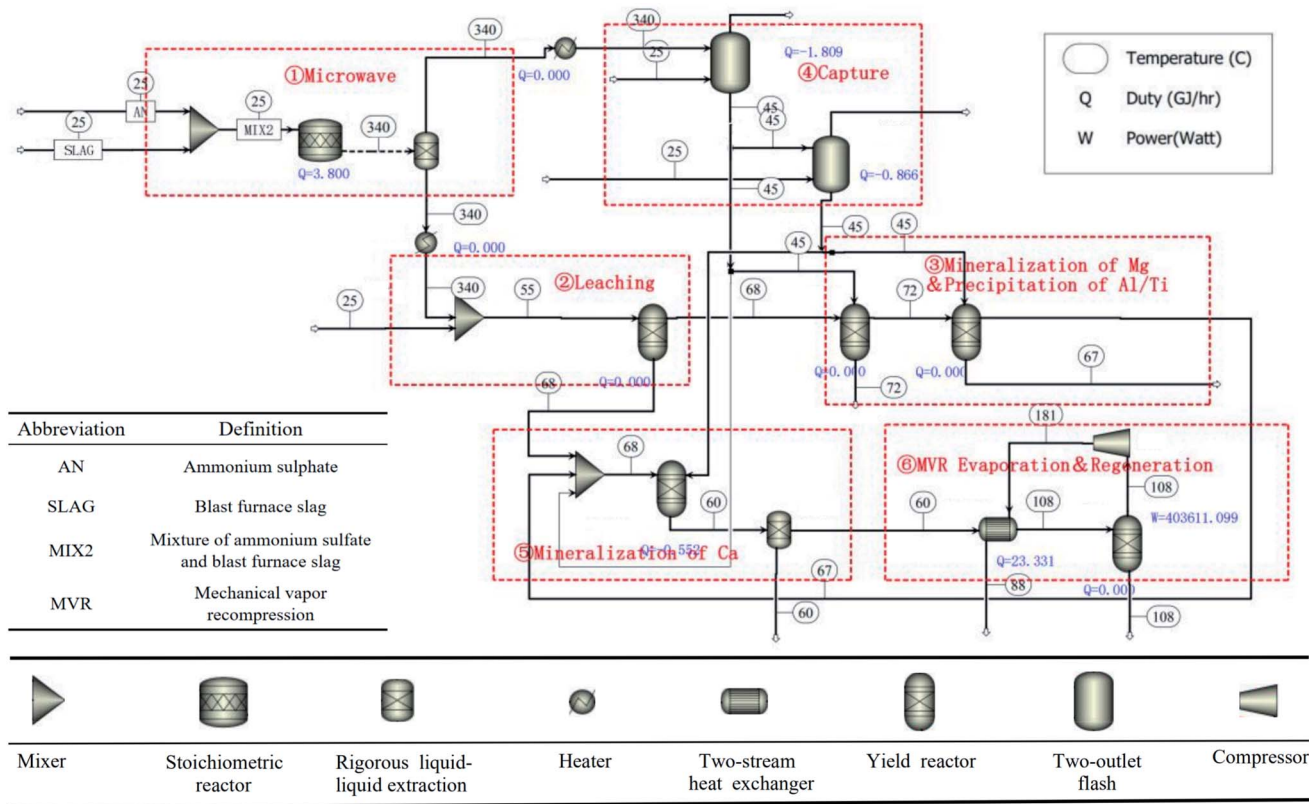


Fig. 11 Schematic of the mineral carbonation process of Ti-bearing BF slag in Aspen Plus v8.8 (① roasting, ② leaching, ③ hydrolysis and crystallization, ④ trapping, ⑤ mineralization, and ⑥ recovery of  $(\text{NH}_4)_2\text{SO}_4$ ).



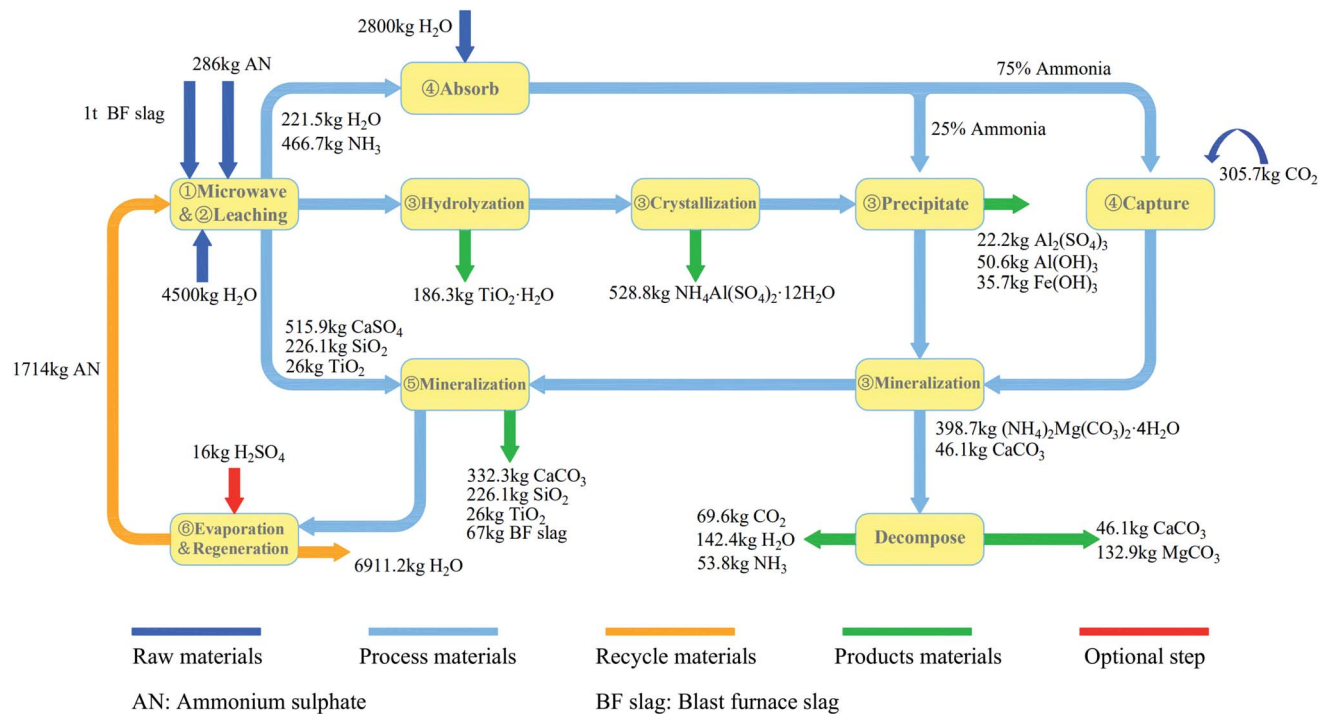


Fig. 12 The material balance of the mineral carbonation process of Ti-bearing BF slag.

calcination, 98 wt% of  $\text{TiO}_2$  could be obtained from the precipitation. After filtration, the leaching solution was directly put into a  $10^\circ\text{C}$  water bath for 12 h, and 62% of Al was precipitated in the form of  $\text{NH}_4\text{Al}(\text{SO}_4)_2 \cdot 12\text{H}_2\text{O}$  (purity of 99%),<sup>31</sup> and 528.8 kg of  $\text{NH}_4\text{Al}(\text{SO}_4)_2 \cdot 12\text{H}_2\text{O}$  could be obtained with 1 ton of BF slag. Then the pH value was adjusted by ammonia produced in the first step, and the remaining  $\text{Al}^{3+}$  and  $\text{Fe}^{3+}$  were precipitated.

Step 4:  $\text{CO}_2$  was captured by ammonia gas from the roasting process to produce ammonium carbonate.

Step 5: Ammonium carbonate was added to the solution to react with  $\text{Ca}^{2+}$ ,  $\text{Mg}^{2+}$ , and  $\text{CaSO}_4$  in leaching residue to produce  $\text{CaCO}_3$  and  $\text{MgCO}_3$ .

Step 6:  $(\text{NH}_4)_2\text{SO}_4$  was recovered from the solution by evaporation.

The simulation calculation of the process showed that 236.1 kg of  $\text{CO}_2$  could be mineralized by one ton of BF slag, which was 86% of the  $\text{CO}_2$  capture potential. The main components of the solid products from the leaching residue mineralization were  $\text{CaCO}_3$  and  $\text{SiO}_2$ , which could be used as raw materials for cement. The final solid products from the leaching solution mineralization were  $\text{CaCO}_3$  and  $\text{MgCO}_3$ , which could replace natural dolomite mining. Through the simulation of the process flow, it could be concluded that the energy consumption of the process was mainly distributed in three processes: roasting, the recovery of  $(\text{NH}_4)_2\text{SO}_4$ , and the capture of  $\text{CO}_2$ . Here, the energy consumption of these three processes was transformed into the energy consumption for mineralizing 1 kg of  $\text{CO}_2$ , to analyze whether microwave roasting could allow saving process energy. The energy consumption of mineralizing

1 kg of  $\text{CO}_2$  in microwave roasting was compared with that in traditional roasting, as shown in Fig. 13, where it can be seen that microwave roasting could accelerate the roasting reaction rate and increase the sulfation ratios of BF slags. Moreover, it could significantly reduce the energy consumption of treating 1 kg of  $\text{CO}_2$  in each unit of the whole process, and the energy consumption for mineralizing 1 kg of  $\text{CO}_2$  could decrease by 20.3 MJ, which represented a 40.2% reduction compared with traditional roasting.

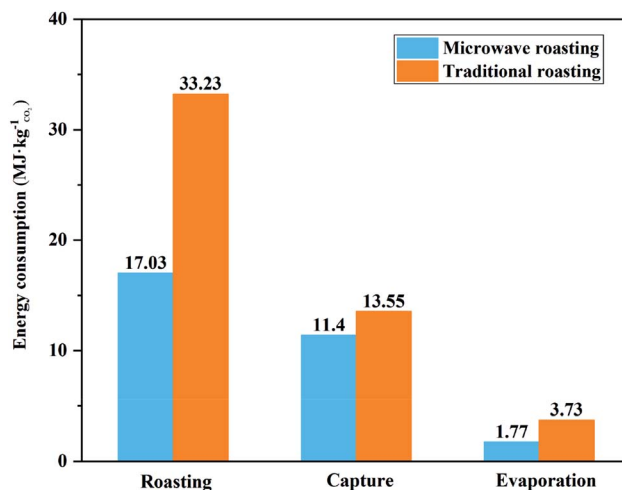


Fig. 13 Comparison of the energy consumption between microwave roasting and traditional roasting.



## 5. Conclusion

This study was focused on microwave roasting and the leaching of BF slag. Under the optimized experimental conditions ( $T = 340\text{ }^{\circ}\text{C}$ , holding time = 2 min), the best sulfation ratios of Ca, Mg, Al, and Ti were 93.3%, 98.3%, 97.5%, and 80.4%, respectively. The main advantage of employing microwave technology was due to the significant reduction in the roasting time and energy saving. The valuable elements in the BF slag were leached out with distilled water, whereby about 57 kg sulfuric acid per ton of BF slag could be saved, and by-products with economic value, such as  $\text{TiO}_2$  (purity of 98%) and  $\text{NH}_4\text{-Al}(\text{SO}_4)_2 \cdot 12\text{H}_2\text{O}$  (purity of 99%), could be obtained. Furthermore, 236.1 kg of  $\text{CO}_2$  could be mineralized by one ton of BF slag. Compared with traditional roasting, the production efficiency of microwave roasting was increased by more than 10 times. Moreover, after simulation with Aspen Plus v8.8 software, the energy consumption for mineralizing 1 kg of  $\text{CO}_2$  could be reduced by 40.2% compared with traditional roasting.

This process could reduce  $\text{CO}_2$  emissions from iron and steel plants, whereby even though all BF slags are used for mineralizing  $\text{CO}_2$ , only a small proportion of  $\text{CO}_2$  emissions from iron and steel industry can be offset. It is difficult for the iron and steel industry to meet the requirements of negative emission in the short term, but the  $\text{CO}_2$  emissions could be further reduced by carbon sequestration in other alkaline wastes (basic oxygen slag, coal ash, etc.). The microwave roasting of BF slag for  $\text{CO}_2$  mineralization was proved to be an energy-efficient method with high productivity and economy, which has broad application prospects in industrial waste treatment and  $\text{CO}_2$  storage.

## Conflicts of interest

There are no conflicts of interest to declare.

## Acknowledgements

This work was supported by the Science and Technology Cooperation Program of Sichuan University and Panzhihua, China [No. 2018CDPZH-24]; the Post doctoral interdisciplinary innovation initiation fund, China [No. 0030704153019]; and the Key Research and Development Program of Sichuan, China [No. 18ZDYF]; the Science and Technology Benefiting Project of Chengdu, China [No. 2016-HM01-00399-SF].

## References

- M. H. Ibrahim, M. H. El-Naas, A. Benamor, S. S. Al-Sobhi and Z. Zhang, *Processes*, 2019, 7, 1–21.
- M. S. Ba-Shammakh, *Energy Fuels*, 2019, 33, 11439–11445.
- P. Renforth, *Nat. Commun.*, 2019, 10, 1401.
- S. Lee, J. W. Kim, S. Chae, J. H. Bang and S. W. Lee, *J. CO<sub>2</sub> Util.*, 2016, 16, 336–345.
- Q. Liu, W. Liu, J. Hu, L. Wang, J. Gao, B. Liang, H. Yue, G. Zhang, D. Luo and C. Li, *J. Cleaner Prod.*, 2018, 197, 242–252.
- H. J. Ho, A. Iizuka and E. Shibata, *Ind. Eng. Chem. Res.*, 2019, 58, 8941–8954.
- S. Eloneva, S. Teir, J. Salminen, C. J. Fogelholm and R. Zevenhoven, *Energy*, 2008, 33, 1461–1467.
- S. Eloneva, A. Said, C. J. Fogelholm and R. Zevenhoven, *Appl. Energy*, 2012, 90, 329–334.
- S. Teir, S. Eloneva, C. J. Fogelholm and R. Zevenhoven, *Appl. Energy*, 2009, 86, 214–218.
- Q. Zhao, C. J. Liu, M. F. Jiang, H. Saxén and R. Zevenhoven, *Miner. Eng.*, 2015, 79, 116–124.
- M. M. Maroto-Valer, D. J. Fauth, M. E. Kuchta, Y. Zhang and J. M. Andrésen, *Fuel Process. Technol.*, 2005, 86, 1627–1645.
- X. Wang and M. M. Maroto-Valer, *Fuel*, 2011, 90, 1229–1237.
- A. Sanna, A. Lacinska, M. Styles and M. M. Maroto-Valer, *Fuel Process. Technol.*, 2014, 120, 128–135.
- A. Sanna, X. Wang, A. Lacinska, M. Styles, T. Paulson and M. M. Maroto-Valer, *Miner. Eng.*, 2013, 49, 135–144.
- J. Fagerlund, E. Nduagu, I. Romão and R. Zevenhoven, *Proc. 23rd Int. Conf. Effic. Cost. Optim. Simulation, Environ. Impact Energy Syst. ECOS 2010*, 2010, vol. 4, pp. 67–75.
- J. Fagerlund, E. Nduagu, I. Romão and R. Zevenhoven, *Front. Chem. Eng. China*, 2010, 4, 133–141.
- O. Rahmani, *J. CO<sub>2</sub> Util.*, 2020, 35, 265–271.
- G. Chu, C. Li, W. Liu, G. Zhang, H. Yue, B. Liang, Y. Wang and D. Luo, *Energy*, 2019, 166, 1314–1322.
- J. Hu, W. Liu, L. Wang, Q. Liu, F. Chen, H. Yue, B. Liang, L. Lü, Y. Wang, G. Zhang and C. Li, *J. Energy Chem.*, 2017, 26, 927–935.
- L. Wang, W. Liu, J. Hu, Q. Liu, H. Yue, B. Liang, G. Zhang, D. Luo, H. Xie and C. Li, *Chin. J. Chem. Eng.*, 2018, 26, 583–592.
- J. Gao, C. Li, W. Liu, J. Hu, L. Wang, Q. Liu, B. Liang, H. Yue, G. Zhang, D. Luo and S. Tang, *Chin. J. Chem. Eng.*, 2019, 27, 157–167.
- M. Al-Harashsheh and S. W. Kingman, *Hydrometallurgy*, 2004, 73, 189–203.
- H. Li, Z. Zhao, C. Xiouras, G. D. Stefanidis, X. Li and X. Gao, *Renewable Sustainable Energy Rev.*, 2019, 114, 109316.
- C. Lucas-Torres, A. Lorente, B. Cabañas and A. Moreno, *J. Cleaner Prod.*, 2016, 138, 59–69.
- Y. Yuan, Y. Zhang, T. Liu, P. Hu and Q. Zheng, *J. Cleaner Prod.*, 2019, 234, 494–502.
- S. Waheed Ul Hasan and F. N. Ani, *Ind. Eng. Chem. Res.*, 2014, 53, 12185–12191.
- C. Yan, N. Yoshikawa and S. Taniguchi, *ISIJ Int.*, 2005, 45, 1232–1237.
- J. Highfield, H. Lim, J. Fagerlund and R. Zevenhoven, *RSC Adv.*, 2012, 2, 6535–6541.
- J. Hu, *Research of the process of CO<sub>2</sub> mineral carbonation with Al<sub>2</sub>O<sub>3</sub> by-product using blast furnace slag and kinetics*, Sichuan University, 2018.
- L. Wang, *A study on the indirect mineral carbonation of titanium-bearing blast furnace slag coupled with recovery of high value-added products of titanium and aluminum*, Sichuan University, 2018.
- C. Wang, *Lab. Sci.*, 2013, 16, 4–6.

